NATIONAL BOARD FOR TECHNICAL EDUCATION
NATIONAL JOURNAL OF TECHNICAL EDUCATION
Volume 23 Nos. 2 2024
ISSN No. 2992-3522

Microwave-Assisted Synthesis of $ZnCl_2$-Activated Carbon from Typha australis Grass: Multi-Response Process Optimisation and Characterisation

A. B. Makama[1]*, M. A. Sadiq [2], and S. A. Saidu [3]

[1]Department of Chemical Engineering Technology, The Federal Polytechnic, Nasarawa
[2]Department of Science Laboratory Technology, The Federal Polytechnic, Nasarawa
[3]Faculty of Applied Science, Federal University, Gashua
* Corresponding author: abmakama@hotmail.com.

Abstract

This study synthesised low-cost activated carbon from *Typha australis* grass via chemical activation with $ZnCl_2$ and microwave heating. The Taguchi L16 design coupled with grey relational analysis optimised the carbon yield and iodine number by adjusting microwave power, irradiation time, $ZnCl_2$ concentration, and soaking time. The optimal conditions were 400W, 20 minutes, 50 vol% $ZnCl_2$, and 12 hours soaking, yielding 43.77% carbon with 798.27mg/g iodine uptake. Characterisation of the *Typha* grass precursor used TGA, proximate, and ultimate analyses. The optimised activated carbon's surface properties were analysed by SEM, FTIR, surface area/porosity, XRD, and point of zero charge measurements. SEM revealed agglomerated spherical particles with void stacking. The carbon exhibited a BET surface area of 424.5m^2/g, micropore volume of 0.164cm^3/g, and presence of acidic functional groups confirmed by a pH_{pzc} of 6.6. FTIR detected various acidic surface groups beneficial for adsorption. XRD indicated an amorphous carbon structure. Overall, the $ZnCl_2$/microwave activation successfully produced a high surface area, microporous carbon from *Typha* biomass with optimal pore structure and surface chemistry for adsorption applications.

[1] abmakama@hotmail.com; Corresponding author
[2] faseediq06@gmail.com
[3] saidusa1960@gmail.com

1. Introduction

Activated carbon (AC) is a material with a unique set of physicochemical properties that include rich functional groups, good chemical stability, high surface area, large porosity, and electrical conductivity, making it a valuable industrial material (Ullah et al., 2024). AC is usually produced from non-renewable, carbon-rich petroleum-based materials like bituminous coal, petroleum residues, peat, lignite, and polymers (Su´arez-Ruiz & Crelling, 2008). However, there is growing interest in using agricultural waste as a green and sustainable alternative to these traditional precursors (Gan, 2021).

The National Institute for Freshwater Fisheries Research (NIFFR, 2002) has documented the widespread invasion of various aquatic weed species including *Typha australis* grass in shallow freshwater bodies in Nigeria. *Typha* grass rapidly colonises and dominates freshwater habitats, posing significant challenges to irrigation farming, fishing, and navigation. Traditional aquatic weed control methods have been largely ineffective, costly, and unsustainable (Uka et al., 2007). Given the limited success of these methods, a new strategy is needed to manage this invasive weed.

In response, we propose utilising *T. australis* leaves as biomass to produce low-cost activated carbon. Repurposing the plant as a valuable bio-resource rather than a nuisance weed will alleviate pressure on traditional AC precursors, and mitigate its rapid proliferation. Moreover, local AC production will reduce reliance on imports and conserve foreign exchange. Previous studies have demonstrated the viability of *Typha* grass for activated carbon (Hanumantharao et al., 2012).

The objective of this study was to optimise the production of activated carbon from the readily available and often invasive *Typha australis* grass biomass using microwave heating and $ZnCl_2$ activation. The goal was to achieve high yield and iodine number, which are desirable quality characteristics for activated carbon. To identify the optimum settings for the operating parameters, the Taguchi method was employed in conjunction with the weighted grey relational analysis technique. The Taguchi-based optimisation method streamlined the experimental process (Bagchi, 1993), while the weighted grey relational analysis facilitated the multi-response optimisation of the desired quality characteristics (Kuo et al., 2008). Comprehensive characterisation of the optimised activated carbon was performed to understand its surface properties and potential applications.

2. Experimental

2.1. Materials

2.1.1. Chemicals and Reagents

The chemicals used in this study - zinc chloride, hydrochloric acid, and sodium hydroxide - were all of analytical grade and obtained from Honeywell agents. Nitrogen gas was supplied by Air Liquide Nigeria Ltd. Double-distilled water was used to prepare all solutions.

2.1.2. Source and Preparation of *Typha australis* Grass

The Typha australis (TL) grass used in this investigation was obtained from Nguru town in the Hadeja-Nguru Wetlands located at Latitude: 12A˚° 38' 59.99" N, Longitude: 10A˚° 35' 17.99" E in Yobe State, Nigeria. Harvested T. australis grass as depicted in Fig. 1(a) was initially cleansed with warm DD water to remove impurities. The washed grass was cut into small pieces measuring (2.5 ± 0.5)cm and left to air dry for 7 days. Following this, the cut biomass was further oven dried overnight at (100 ± 2)◦C. The dried sample underwent multiple washings with DD-water and dried again at (110 ± 2)◦C for 5h in an oven. The resulting biomass as shown in Fig. 1(b) was then milled into fine powder and screened to yield prolate particles ranging in size from 0.5mm to 1.0mm size as shown in Fig. 1(c). The screened T. australis powder (TAP) was subsequently stored in a sealed container and used later for characterisation and synthesis of activated carbon.

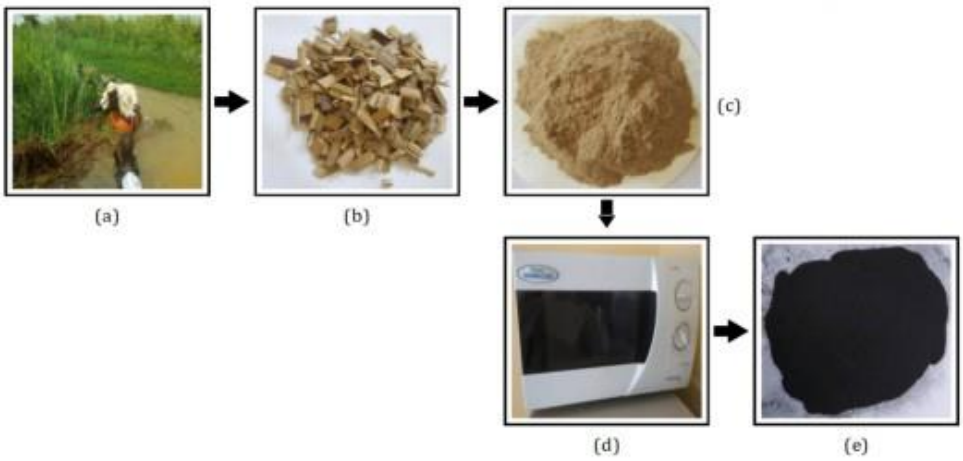

Figure 1: Production of activated carbon from *T. australis* grass. (a) grass harvesting from Nguru wetlands, (b) cut and dried grass, (c) *T. australis* grass powder, (d) microwave oven, and I activated carbon. Adapted form Sadiq et al., 2020.

2.2. Characterisation of *T. ausralis* Grass

2.2.1. Proximate and Ultimate analyses

The assessment of the physicochemical composition of a biomass typically involves proximate and ultimate analyses. Proximate analysis entails determining the levels of ash, moisture (M), and volatile matter (VM). The sum of these components subtracted from 100 yields the fixed carbon (FC) percentage. On the other hand, ultimate analysis provides insight into the elemental makeup of the biomass, including C, H_2, N_2, and O_2. In this study, proximate and ultimate analyses were conducted according to ASTM Standard D5142-02 (2017) and ASTM Standard D5373-02 (2017), respectively. Elemental analyser model (LECO CHNS 628) was used for ultimate analysis. Oxygen content of the biomass was obtained by deducting the combined percentages of carbon, hydrogen, and nitrogen from 100%.

2.2.2. Thermogravimetric Analysis

The thermal stability and phase transitions of *T. australis* grass were observed by thermogravimetric analysis. The Thermogravimetric Analysis STA-8000, Perkin Elmer brand was used for this pyrolysis experiment.

2.3. Synthesis of Activated Carbon from T. australis Grass

2.3.1. Synthesis

The activated carbon production involved two main steps. First, 25g *T. australis* powder was soaked in 500mL $ZnCl_2$ solution under stirring (100 rpm) at 60°C for a specified, allowing $ZnCl_2$ impregnation. Second, 5g of the impregnated powder was carbonised by microwave irradiation under N_2 gas flow ($150cm^3\ min^{-1}$), after 5min oven preheating. The $ZnCl_2$ concentration, microwave power, irradiation time, and soaking time are adjusted according to the Taguchi design matrix given in Table III. The AC produced was leached with 0.1M HCl for 4h to remove residual $ZnCl_2$, rinsed many times with DD-water till wash-water pH remains constant and oven dried at 105°C overnight. Finally, the dried AC is designated as *Typha australis* powder activated carbon (TPAC)

Table I: L16 Control factors and their levels.

		Factor Levels			
Factors	Symbols	1	2	3	4
Microwave Radiation Power (W)	A	300	400	500	600
Irradiation Time (min)	B	10	15	20	25
$ZnCl_2$ Concentration (Vol.%)	C	30	40	50	60
Soaking Time (h)	D	6	12	18	24

2.4. Optimising of Process Conditions

2.4.1. Taguchi Design Matrix

In this research, the Taguchi method was utilised to design experimental matrix for the production of $ZnCl_2$-activated carbon from *T. australis* grass. Taguchi design employs fractional factorial design to investigate how control factors affect response variables and identify the best operating conditions efficiently. It uses orthogonal arrays and statistical analysis to minimise the number of experiments needed to pinpoint key operational factors (Bagchi, 1993). A Taguchi L_{16} orthogonal array design with four controllable factors, each with four levels was selected and used to determine the optimised factor settings. The selected parameters and their levels are shown in Table I. Carbon yield (Y_1, %) and its iodine uptake number (Y_2, mg/g) were selected as quality characteristics to be maximised. The activated carbon yield was estimated according to Eq. (1) while its iodine adsorption capacity was determined according to ASTM Standard D4607-14 (2021). *Design Expert* statistical software version 6 was used to design the Taguchi experimental array. The complete design matrix including the obtained values for the Y_1 and Y_2 are summarised in Table II.

$$Y_1(\%) = \frac{Mass\ of\ AC}{Mass\ of\ Precursor} \times 100 \quad (1)$$

2.4.2. Grey Relational Analysis

The weighted grey relational analysis (WGRA) method was utilised to perform the multi-response optimisation of the desired quality characteristics (carbon yield and iodine number). The response data given in Table II was processed using a series of Eqs. (2) to (7) to compute the signal-to-noise ratios (SNRs), normalise the SNRs, calculate the grey relational coefficients, determine the weight factors, and ultimately obtain the grey relational grades. This optimisation procedure followed the notations and steps outlined by Kuo et al. (2008) and Yan and Li (2013), which involve:

Table II: L16 orthogonal design matrix with factors and responses.

		Factors				Response	
Std	Run	A (W)	B (min)	C (Vol.%)	D (h)	Y1 (%)	Y_2(mg/g)
11	1	500	20	30	12	37.58	766.90
12	2	500	25	40	6	39.38	751.76
14	3	600	15	50	6	39.62	775.60
4	4	300	25	60	24	40.96	767.39
5	5	400	10	40	18	31.02	767.58
3	6	300	20	50	18	42.09	805.53
1	7	300	10	30	6	24.96	738.40
8	8	400	25	50	12	43.97	891.77
9	9	500	10	50	24	35.03	793.17
7	10	400	20	60	6	45.52	848.04
15	11	600	20	40	24	38.61	768.95
16	12	600	25	30	18	37.57	734.02
10	13	500	15	60	18	41.97	770.59
6	14	400	15	30	24	38.79	769.45
2	15	300	15	40	12	35.41	755.61
13	16	600	10	60	12	31.78	747.63

1. Calculating the SNRs (η_{ij}) for each response.

$$SNR\left(\eta_{ij}\right) = -10log\left(\frac{1}{n}\sum_{i=1}^{n}\frac{1}{y_{ij}{}^{2}}\right) \quad (2)$$

2. Normalising the SNRs (Z_{ij}) to allow comparison across different units.

$$Z_{ij} = \frac{\eta_{ij} - min\{\eta_{ij}\}_{j=1}^{m}}{max\{\eta_{ij}\}_{j=1}^{m} - min\{\eta_{ij}\}_{j=1}^{m}} \quad (3)$$

3. Computing the grey relational coefficients (GRC, $\gamma(y_o(k),y_i(k))$) based on the normalised SNRs.

$$\gamma\left(y_o(k), y_i(k)\right) = \frac{\Delta_{min}+\xi\Delta_{max}}{\Delta_{oj}(k)+\xi\Delta_{max}} \quad (4)$$

4. Assigning weight factors (ω) to each response based on their relative importance.

$$R_{ij} = max\{K_{ij1}, K_{ij2}, \dots, K_{ijk}\} - min\{K_{ij1}, K_{ij2}, \dots, K_{ijk}\} \quad (5)$$

$$\omega = \frac{\sum_{j=1}^{p} R_{ij}}{\sum_{i=1}^{m}\sum_{j=1}^{p} R_{ij}} \quad (6)$$

(6)

5. Determining the overall grey relational grade (WGRG, γ_j) by combining the weighted GRC.

$$\Upsilon_j = \sum_{j=1}^{m} \omega_k \gamma_{ij} \quad (7)$$

Where the variables are defined as follows:

- j ranges from 1 to p, where p is the total number of experimental data points.
- k ranges from 1 to m, where m is the number of response variables.
- $y_o(k)$ represents the reference sequence, with $y_o(k) = 1 \forall k$.
- $y_j(k)$ represents the comparison sequence for a specific experiment j.
- $\Delta_{oj} = |y_o(k) - y_j(k)|$: This is the absolute difference between the reference ($y_o(k)$) and comparison sequences ($y_j(k)$).
- $\Delta_{min} = \min_{j\in J}(\min_k(|y_o(k) - y_j(k)|))$: The smallest difference across all j and k.
- $\Delta_{max} = \max_{j\in J}(\max_k(|y_o(k) - y_j(k)|))$: The largest difference across all j and k.
- Lastly, ξ is the distinguishing coefficient, which ranges from 0 to 1 ($0 \leq \xi \leq 1$).

The grey relational grade serves as the multi-response performance index, where higher values indicate the optimal parametric combination for maximising the desired responses simultaneously. This systematic approach enables the effective optimisation of multiple quality characteristics concurrently.

Result of weighted grey relational analysis of the response data is presented in Table III.

Table III: *Results of grey relational analysis*

[a]η_{ij}		[b]Z_{ij}		Δ_{oj}		[c]$\gamma(y_o(k), y_i(k))$		
Y_1	Y_2	Y_1	Y_2	Y_1	Y_2	Y_1	Y_2	[d]$\bar{y}_{ij}$
31.499	57.695	0.681	0.225	0.319	0.775	0.758	0.563	0.658
31.906	57.522	0.759	0.123	0.241	0.877	0.806	0.533	0.665
31.958	57.793	0.769	0.283	0.231	0.717	0.812	0.582	0.694
32.247	57.700	0.824	0.228	0.176	0.772	0.851	0.564	0.703
29.833	57.702	0.362	0.230	0.638	0.770	0.610	0.565	0.587
32.484	58.122	0.870	0.478	0.130	0.522	0.885	0.657	0.767
27.945	57.366	0.000	0.031	1.000	0.969	0.500	0.508	0.504
32.863	59.005	0.942	1.000	0.058	0.000	0.945	1.000	0.974
30.889	57.987	0.564	0.398	0.436	0.602	0.696	0.624	0.659
33.164	58.568	1.000	0.742	0.000	0.258	1.000	0.795	0.894
31.734	57.718	0.726	0.239	0.274	0.761	0.785	0.568	0.673
31.497	57.314	0.681	0.000	0.319	1.000	0.758	0.500	0.625
32.459	57.736	0.865	0.250	0.135	0.750	0.881	0.571	0.721
31.774	57.724	0.734	0.242	0.266	0.758	0.790	0.569	0.676
30.983	57.566	0.582	0.149	0.418	0.851	0.705	0.540	0.620
30.043	57.474	0.402	0.094	0.598	0.906	0.626	0.525	0.574

[a] η_{ij}: Signal-to-noise-ratio defined in Eq. (2).

[b] Z_{ij}: Normalised SNR defined in Eq. (3)

[c] $\gamma(y_o(k),y_i(k))$: Grey relational coefficient defined in Eq. (4)

[d] γ_j: Weighted grey relational grades defined in Eq. (7)

2.5. Characterisation of TPAC Synthesised Under Optimal Operating Conditions

The surface area and pore structure were analysed using N_2 adsorption-desorption measurements

(3Flex, Micromeritics, USA). Scanning electron microscopy (SEM) (S4800, Hitachi, Japan) examined the morphology. X-ray diffraction patterns were obtained (Rigaku D/Max 2500, CuK_α radiation, 20° to 80° range). Fourier-transform infrared spectroscopy (Nicolet 6700, Thermo Nicolet) analysed functional groups in the $500cm^{-1}$ to $4000cm^{-1}$ range. For zeta potential, 0.1 mg adsorbent was added to 50 mL distilled water, pH adjusted from 4.0 - 10.0 using HCl/NaOH. The point of zero charge (pH_{PZC}) was determined as the pH where final pH equaled initial pH after contact time (Lopez-Ramon et al., 1999).

3. Results and Discussions

3.1. Characterisation of *T. australis* Grass

Table IV: Proximate and ultimate analyses results for *T. australis* powder compared with literature data (%, Dry basis).

	Proximate				Ultimate					
Biomass	Ash	FC[a]	M[b]	VM[c]	C	H	N	S	O[d]	Reference
TA[e]	6.15	17.90	2.34	73.61	50.72	5.81	1.30	0.32	41.85	This work
Tan[f]	3.81	2.18	13.95	80.06	52.90	5.84	1.22	-	40.04	Singh et al. (2017)
EC[g]	20.80	2.80	6.80	70.50	33.10	5.33	0.9	0.2	60.6	Sahoo et al. (2019)
SA[h]	6.78	-	-	-	46.70	6.10	0.15	-	42.30	Wang et al. (2011)
Corncob	2.38	10.85	4.19	82.58	38.55	5.57	0.42	0.58	48.31	Feng et al. (2020)

[a] FC: Fixed carbon [b] M: Moisture [c] VM: Volatile matter [d] By difference [e] TA: *Typha australis* [f] Tan: *Typha angustifolia* [f] EC: *Eichhornia crassipes* [h] SA: *Spartina alterniflora*

3.1.1. Proximate and Ultimate Analyses

The proximate result in Table IV revealed *T. australis* grass composition as 6.15% ash, 17.90% fixed carbon, 2.34% moisture, and 73.61% volatile matter. Comparing to other biomasses, *T. australis* had higher ash than *Typha angustifolia* and corncob but lower than *Eichhornia crassipes* and *Spartina alterniflora*. Its volatile matter was lower than *Typha angustifolia* and corncob but higher than *Eichhornia crassipes*. Furthermore, the fixed carbon content was higher than *Eichhornia crassipes* and corncob but lower than *Typha angustifolia*. As biomass with high carbon and low ash is ideal for activated carbon production (Moralı et al., 2018), the relatively high carbon and low ash of *T. australis* confirm its suitability.

The ultimate analysis (Table IV) showed *T. australis* comprised 50.72% C, 5.81% H, 1.30% N, 0.32% S, and 41.85% O. Compared to other aquatic weeds and corncob, *Eichhornia crassipes* had the lowest carbon, while *Spartina alterniflora*

was highest. *T. australis* and *Typha angustifolia* had similar carbon levels, with corncob in between. Hydrogen was highest in *Spartina alterniflora* and lowest in *Eichhornia crassipes*. Nitrogen and sulfur varied, with *Spartina alterniflora* lowest in N and *Eichhornia crassipes* lowest in S. Oxygen was highest in *Eichhornia crassipes* and lowest in *Typha angustifolia*. Although slight differences existed versus literature, the *T. australis* values fell within typical aquatic weed ranges.

3.1.2. Thermogravimetric Analysis

Figure 2 gives the TGA/ DTG thermal degradation characteristics of the *T. australis* grass feedstock in a N_2 atmosphere. The decomposition of *T. australis* grass takes place in two stages. First, moisture loss of about 1.75% occurred in a narrow temperature range of 100°C–110°C and yields a sharp, single DTG peak at 108.56°C. Second, the hemicellulose degradation region occurred between 248°C–310°C. The sample lost most of its residual mass (about 67.51 %) in this region. Third, the degradation at >360°C could be attributed to the gradual devolatilisation of lignin (Bajpai, 2018). The DTG curve shows the temperatures (108°C, 271°C and 343°C) at which maximum rates of mass loss ($-0.50\%min^{-1}$, $-7.17\%min^{-1}$ and $-0.88\%min^{-1}$) occurred during the moisture drying, hemicellulose, and lignin devolatilisation stages, respectively. During the TG analysis from 50°C–600°C, the *T. australis* grass lost about 71.41 % of its initial mass.

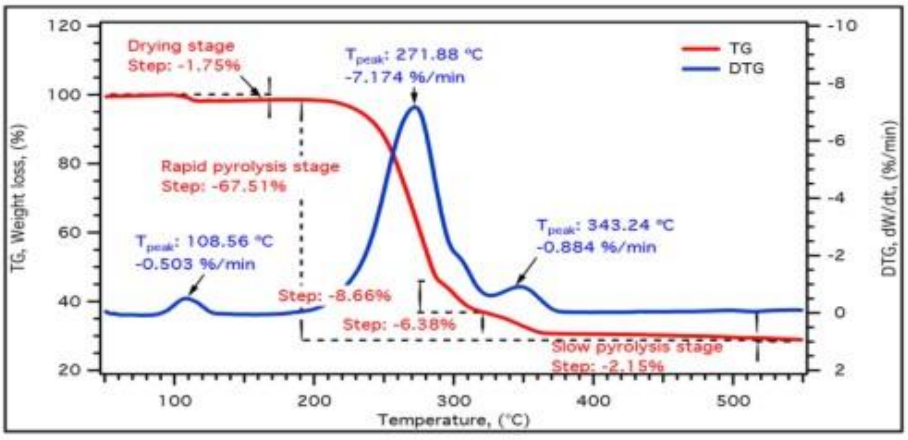

Figure 2: TGA and DTG thermograms of *T. australis* grass.

3.2. Multi-Response Optimisation of TPAC Synthesis Conditions

To achieve optimal production of activated carbon with maximised yield and iodine number, it is crucial to aim for the highest possible Grey Relational Grade (GRG) value (Yan & Li, 2013). Thus, a "larger-is-better" criterion was applied in the Taguchi design. Table III presents the mean GRG response values for different control factors and their levels. The optimal settings (bold values in Table III) were determined based on the highest GRG value at each factor level. These values are graphically illustrated in Fig. 3(a).

Table V: *Grey relational grade response table.*

Level	A	B	C	D
1	0.649	0.581	0.616	0.689
2	**0.783**	0.678	0.636	**0.706**
3	0.676	**0.748**	**0.773**	0.675
4	0.641	0.742	0.723	0.678
Delta	0.141	0.167	0.158	0.031
Rank	3	1	2	4

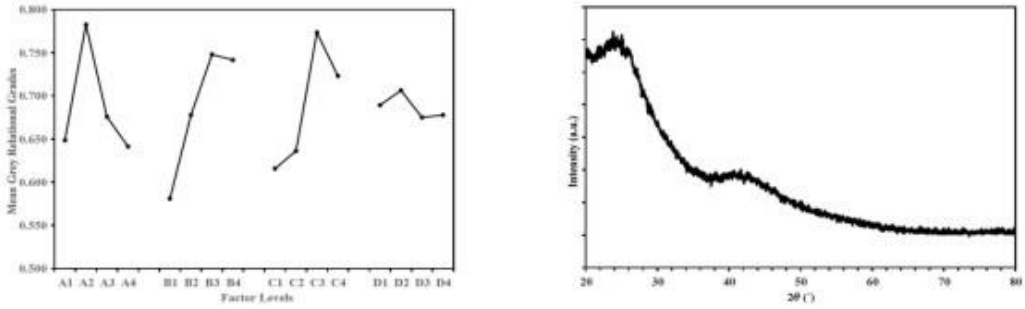

Figure 3: (a) Response graph for mean grey relational grades. (A) Microwave radiation power, (B) irradiation time, (C) concentration of $ZnCl_2$, and (D) Soaking time. (b) Powder X-ray diffraction pattern of TPAC synthesised at the optimised operating conditions.

3.2.1. Optimised Control Factors Settings

The analysis identified the optimal settings as 400W microwave power (Level 2), 20 min irradiation time (Level 3), 50 vol.% $ZnCl_2$ concentration (Level 3), and 12h soaking time (Level 2) to maximise activated carbon yield and iodine number.

Notably, these optimal conditions were not among the 16 experimental runs, demonstrating the efficiency of the Grey Relational Analysis (GRA) design approach (Yan & Li, 2013). The delta statistics of the GRG values indicated the relative significance of each parameter, with irradiation time being most critical, followed by $ZnCl_2$ concentration, microwave power, and soaking time in descending order of impact. Under the optimised settings, the synthesised activated carbon from T. australis (TPAC) achieved an iodine number of 892.31 mg/g and yield of 35.78%, confirming the effectiveness of the approach.

3.3. Characteristics of the TPAC Synthesised Under Optimised Conditions

3.3.1. XRD Analysis

The X-ray diffraction (XRD) profile of the $ZnCl_2$-activated T. australis carbon (TPAC), shown in Fig. 3(b), exhibited two broad Bragg peaks at around 2θ = 24.05° and 42.06°. The peak at 24.05° corresponds to the (002) plane reflection, which is characteristic of disordered aromatic carbon structures. Another peak at 42.06° can be attributed to (100) plane reflection from the hexagonal graphite structure (Canales-Flores & Prieto-Garc´ıa, 2020). Notably, the prominent peak around 24° suggests the predominance of an amorphous carbon structure in the TPAC sample (Mochizuki et al., 2022). Similar XRD profiles have been reported in the literature for activated carbons (Benmahdi et al., 2021).

3.3.2. Surface Morphological and Elemental Analyses

The surface structure of the TPAC sample was assessed using scanning electron microscopy (SEM), as illustrated in Fig. 4(a)-(c). The SEM images at different magnifications (5kx, 20kx, 100kx) revealed that the sample consisted of agglomerated sphere-like particles ranging from 50 nm to 150 nm in diameter. A closer inspection indicated that the stacking of these spherical particles produced numerous pores, cracks and slits, which can potentially enhance the specific surface area of the carbon sample. The surfaces of the sphere-like particles appeared crack-free at the highest magnification shown in Fig. 4(c), suggesting that the TPAC could be thermally and morphologically stable after the $ZnCl_2$ activation and carbonisation process. Similar morphological features have been reported for polypyrrole-based porous carbon activated with $ZnCl_2$ (Li et al., 2020). EDX analysis (Fig. 4) showed that TPAC had a high carbon content, with an atomic fraction of 80.98%. This high carbon content indicates that the $ZnCl_2$

activating agent effectively acted as a dehydrating agent (Benmahdi et al., 2021), facilitating almost complete carbonisation of the sample. Additionally, trace amounts of zinc and chlorine detected on the TPAC surface could be residues from the activation process (Tuli et al., 2020).

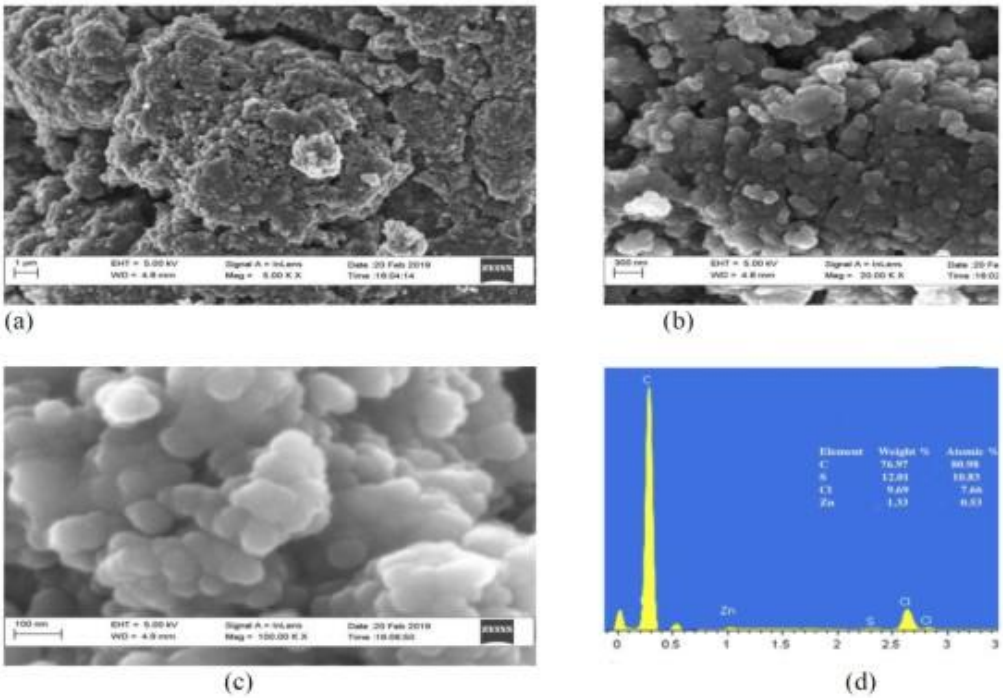

Figure 4: Scanning electron micrograph images at different magnifications (a) - (c) and Energy dispersive spectroscopy (EDS) spectra of TPAC synthesised under optimised operating conditions.

3.3.3. Analysis of Surface Area and Pore Size Distribution

The N_2 adsorption-desorption isotherm at 77K for the synthesised TPAC (Fig. 5(a)) exhibited a Type
IV isotherm (Bardestani et al., 2019), which is characteristic of high surface area mesoporous materials. The study found that the mean pore diameter of TPAC was 2.65 nm, as shown in Fig. 5(b). This small pore size suggests that TPAC contains a large number of micropores. The BET surface area of TPAC was consistent with previous findings for activated carbons derived from *Typha angustata* grass (Hanumantharao et

al., 2012). Table VI summarises the key porous structure properties of the synthesised TPAC as determined by BET and BJH methods. The N_2 adsorption-desorption analysis and the derived textural properties indicate that the synthesis method successfully produced a high surface area, microporous carbon from *T. australis* grass using microwave heating and $ZnCl_2$ activation.

Table VI: Textural characterisations of TPAC synthesised at optimised conditions.

Sample	S_{BET} (mg/g)	V_{mic} (cm^3 /g)	V_{meso} (cm^3 /g)	V_{tot} (cm^3 /g)	D_P (nm)	Y_1 (%)	Y_2 (mg/g)
TPAC	424.5	0.164	0.074	0.238	2.65	43.77	798.27

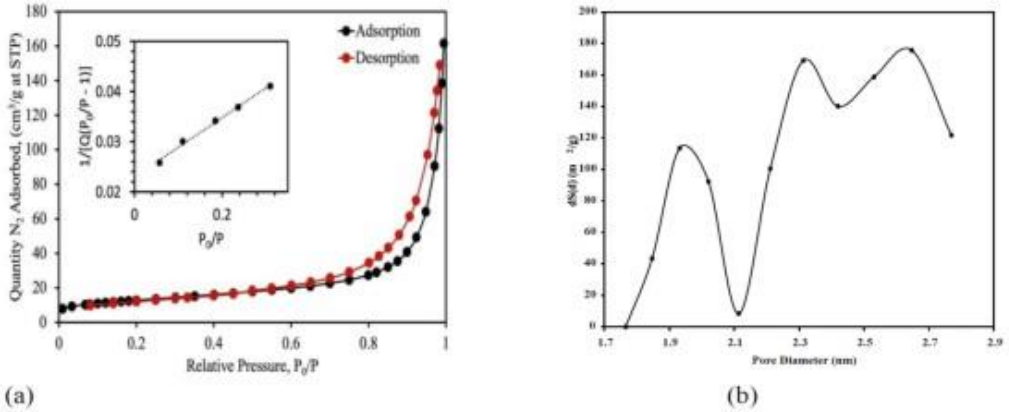

(a) (b)

Figure 5: (a) Adsorption/desorption isotherm of N_2 at −196°C and (b) DFT Pore size distribution of TPAC synthesised at optimised conditions.

3.3.4. FTIR Analysis

Fourier-transform infrared (FTIR) spectroscopy was employed to analyse the surface functional groups present on the *T. australis* carbon (TPAC), as shown in the spectrogram in Fig. 6(a). Several distinctive peaks were observed. A peak at 3407cm^{-1} corresponds to O–H stretching vibration from hydroxyl containing functional groups and those involved in H_2 bonding (Dai et al., 2023). Saturated aliphatic C–H bonds symmetric and asymmetric stretching oscillations were observed at 2941cm^{-1}, (Nath et al., 2013). CH_2 and CH bonds were identified at 2925cm^{-1} and 2851cm^{-1} (Debbarma et al., 2020). Additionally, a peak at 2300cm^{-1} attributed to stretching vibrations of O=C=O groups (Liu et al., 2020). The peak at 1756cm^{-1} indicate the presence of aromatic peroxide groups assigned to C–O stretching vibrations according to Moreno-Castilla et al. (2000). Furthermore, peaks at 1570cm^{-1}, 1144cm^{-1} and 826cm^{-1} correspond to C=C, C-O, and C-H stretching oscillations, respectively

(Ravindran et al., 2023). The peaks at 1144cm^{-1} and 1079cm^{-1} corresponds to stretching oscillations from alcoholic C–O and C–N. The FTIR analysis indicated that the synthesised TPAC contained various oxygenated functional groups, such as –OH and C—O groups, which could act as active sites for interaction with adsorbate molecules.

3.3.5. Zeta Potential

Figure 6(b) presents the zeta-potential plot of the TPAC sample produced under optimised conditions, showing a point of zero charge (pH_{PZC}) of 6.6. This indicates that acidic groups dominate over basic groups on the surface of the activated carbon. Consequently, the TPAC surface is expected to be negatively charged when the solution pH is greater than 6.6, and positively charged when it is less than 6.6. The acidic nature of the TPAC surface is due to carboxylic functional groups formed through complex hydrolysis reactions between $ZnCl_2$ and the precursor material under acidic conditions (Boudrahem et al., 2011). Similar acidic surface charge condition has been reported for $ZnCl_2$-activated carbons (Benmahdi et al., 2021).

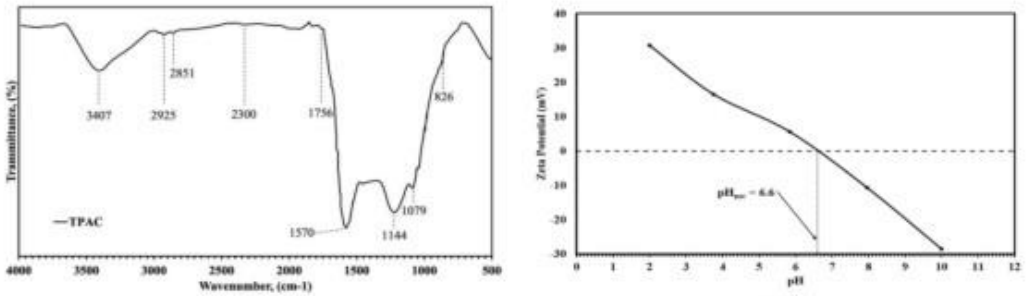

Figure 6: Chart showing: (a) FTIR spectrum and (b) Zeta potential curves versus pH of the $ZnCl_2$-activated carbon (TPAC) synthesised at optimised conditions.

4. Conclusion

Typha australis grass from Hadejia-Nguru Wetlands was utilised as a low-value precursor to synthesise powdered activated carbon via chemical activation with $ZnCl_2$ under microwave heating. The Taguchi method coupled with weighted grey relational analysis optimised the process parameters to maximise activated carbon yield and iodine number. Irradiation time and $ZnCl_2$ concentration were identified as the most significant factors influencing yield and iodine adsorption. The optimal conditions were 400 W microwave power, 20 min irradiation, 50 vol% $ZnCl_2$, and 12 h soaking time. Using these optimised conditions, the synthesis process achieved a yield of 43.77% TPAC from the starting material. Furthermore, the iodine number of the synthesised carbon was measured to

be 798.27mgg^{-1}, indicating its high adsorption capacity and large surface area. Characterisation revealed TPAC had a microporous structure with 424.5m^2 g^{-1} BET surface area and 0.164cm^3 g^{-1} micropore volume. SEM confirmed its porous morphology, while FTIR detected various surface functional groups, beneficial for adsorption applications.

In summary, the study optimised $ZnCl_2$/microwave activation of *Typha* biomass to produce a high-quality microporous activated carbon with excellent yield and adsorption capacity.

Acknowledgement

The researchers express their gratitude to the Tertiary Education Trust Fund (TETFund) for financially supporting this investigation through the Institutional Based Research (IBR) grant awarded. Additionally, they extend their appreciation to the Federal Polytechnic, Nasarawa, for providing the necessary workspace and facilities to conduct this research work.

References

ASTM Standard D4607-14. (2021). Standard test method for determination of iodine number of activated carbon.

ASTM Standard D5142-02. (2017). Standard test methods for proximate analysis of the analysis sample of coal and coke by instrumental procedures.

ASTM Standard D5373-02. (2017). Standard test methods for instrumental determination of carbon, hydrogen, and nitrogen in laboratory samples of coal and coke.

Bagchi, T. P. (1993). *Taguchi methods explained: Practical steps to robust design*. Prentice-Hall.

Bajpai, P. (2018). Wood and fiber fundamentals. In P. Bajpai (Editor), *Biermann's handbook of pulp and paper* (Third Edition, Pages 19–74). Elsevier.

Bardestani, R., Patience, G. S., & Kaliaguine, S. (2019). Experimental methods in chemical engineering: Specific surface area and pore size distribution measurements—bet, bjh, and dft. *Can. J. Chem. Eng.*, *97*(11), 2781–2791.

Benmahdi, F., Oulmi, K., Khettaf, S., Kolli, M., Merdrignac-Conanec, O., & Mandin, P. (2021). Synthesis and characterization of microporous granular activated carbon from silver berry seeds using $ZnCl_2$ activation. *Fuller Nanotub Car N*, *29*(9), 657–669.

Boudrahem, F., Soualah, A., & Aissani-Benissad, F. (2011). Pb(II) and Cd(II) removal from aqueous solutions using activated carbon developed from coffee

residue activated with phosphoric acid and zinc chloride. *J. Chem. Eng. Data*, *56*(5), 1946–1955.

Canales-Flores, R., & Prieto-Garc´ıa, F. (2020). Taguchi optimization for production of activated carbon from phosphoric acid impregnated agricultural waste by microwave heating for the removal of methylene blue. *Diam Relat Mater*, *109*, 108027.

Dai, F., Zhuang, Q., Huang, G., Deng, H., & Zhang, X. (2023). Infrared spectrum characteristics and quantification of OH groups in coal. *ACS Omega*, *8*(19), 17064–17076.

Debbarma, J., Mandal, P., & Saha, M. (2020). N-graphene oxide and N-reduced graphene oxide from jujube seeds: Chemistry and mechanism. *Fuller. Nanotub. Car N*, *28*, 1–5.

Feng, P., Li, J., Wang, H., & Xu, Z. (2020). Biomass-based activated carbon and activators: Preparation of activated carbon from corncob by chemical activation with biomass pyrolysis liquids. *ACS Omega*, *5*(37), 24064–24072.

Gan, Y. X. (2021). Activated carbon from biomass sustainable sources. *C*, *7*(2), 39.

Hanumantharao, Y., Kishore, M., & Ravindhranath, K. (2012). Characterization and defluoridation studies of active carbon derived from typha angustata plants. *J. Anal. Sci. Technol.*, *3*(2), 167–181.

Kuo, Y., Yang, T., & Huang, G.-W. (2008). The use of grey relational analysis in solving multiple attribute decision-making problems. *Comput Ind Eng*, *55*(1), 80–93.

Li, B., Hu, J., Xiong, H., & Xiao, Y. (2020). Application and properties of microporous carbons activated by $ZnCl_2$: Adsorption behavior and activation mechanism. *ACS Omega*, *5*(16), 9398–9407.

Liu, N., Liu, Y., Zeng, G., Gong, J., Tan, X., JunWen, Liu, S., Jiang, L., Li, M., & Yin, Z. (2020). Adsorption of 17β-estradiol from aqueous solution by raw and direct/pre/post-KOH treated lotus seedpod biochar. *J Environ Sci*, *87*, 10–23.

Lopez-Ramon, M., Stoeckli, F., Moreno-Castilla, C., & Carrasco-Marin, F. (1999). On the characterization of acidic and basic surface sites on carbons by various techniques. *Carbon*, *37*(8), 1215–1221.

Mochizuki, Y., Bud, J., Byambajav, E., & Tsubouchi, N. (2022). Preparation and evaluation of activated carbon from low-rank coal via alkali activation and its fundamental CO_2 adsorption capacity at ambient temperature under pure pressurized CO_2. *React. Chem. Eng.*, *7*, 1429–1446.

Moralı, U., Demiral, H., & S¸ens¨oz, S. (2018). Optimization of activated carbon production from sunflower seed extracted meal: Taguchi design of experiment

approach and analysis of variance. *J Clean Prod*, *189*, 602–611.

Moreno-Castilla, C., Lo´pez-Ramo´n, M. V., & Carrasco-Mar´ın, F. (2000). Changes in surface chemistry of activated carbons by wet oxidation. *Carbon*, *38*, 1995–2001.

Nath, K., Panchani, S., Bhakhar, M. S., & Chatrola, S. (2013). Preparation of activated carbon from dried pods of prosopis cineraria with zinc chloride activation for the removal of phenol. *Environ Sci Pollution Res*, *20*(6), 4030–4045.

NIFFR. (2002). *National Surveys of Infestation of Water Hyacinth, Typha Grass and other notious weeds in Water Bodies of Nigeria* (NIFFR Occational Paper Number 5). National Institute for Freshwater Fisheries Research. New Bussa, Nigeria.

Ravindran, B., Nguyen, D. V., Nguyen, H. M., Bui, Q. L. N., Do, T. V. T., Lam, H. H., Tran-Thuy, T.-M., & Nguyen, L. Q. (2023). Magnetic activated carbon from zncl$_2$ and fecl$_3$ coactivation of lotus seedpod: One-pot preparation, characterization, and catalytic activity towards robust degradation of acid orange 10. *Bioinorg Chem Appl*, *2023*, 3848456.

Sadiq, M. A., Sariki, Y. G., Umar, M., & Makama, A. B. (2020). Taguchi optimization of activated carbon production from $ZnCl_2$ impregnated typha grass using microwave heating. *Proceedings of Material Science and Technology Society of Nigeria*.

Sahoo, D., Awasthi, A., Dhyani, V., Biswas, B., Kumar, J., Reddy, Y. S., Adarsh, V., Puthiyamadam,

A., Mallapureddy, K. K., Sukumaran, R. K., Ummalyma, S. B., & Bhaskar, T. (2019). Valueaddition of water hyacinth and para grass through pyrolysis and hydrothermal liquefaction. *Carbon Resour. Convers.*, *2*(3), 233–241.

Singh, Y. D., Mahanta, P., & Bora, U. (2017). Comprehensive characterization of lignocellulosic biomass through proximate, ultimate and compositional analysis for bioenergy production. *Renew. Energy*, *103*, 490–500.

Su´arez-Ruiz, I., & Crelling, J. C. (2008). Coal-derived carbon materials. In I. Su´arez-Ruiz & J. C. Crelling (Editors), *Applied coal petrology: The role of petrology in coal utiliztion* (Pages 193–225). Elsevier.

Tuli, F., Hossain, A., Kibria, A. F., Tareq, A., Mamun, S., & Ullah, A. A. (2020). Removal of methylene blue from water by low-cost activated carbon prepared from tea waste: A study of adsorption isotherm and kinetics. *Environ. Nanotechnol. Monit. Manag.*, *14*, 100354.

Uka, U. N., Chukwuka, K., & Daddy, F. (2007). Water hyacinth infestation and

management in nigeria inland waters: A review. *J Plant Sci*, *2*, 480–488.

Ullah, S., Shah, S. S. A., Altaf, M., Hossain, I., El Sayed, M. E., Kallel, M., El-Bahy, Z. M., ur Rehman, A., Najam, T., & Nazir, M. A. (2024). Activated carbon derived from biomass for wastewater treatment: Synthesis, application and future challenges. *J Anal Appl Pyrol*, 106480.

Wang, Z., Nie, E., Li, J., Zhao, Y., Luo, X., & Zheng, Z. (2011). Carbons prepared from spartina alterniflora and its anaerobically digested residue by h3po4 activation: Characterization and adsorption of cadmium from aqueous solutions. *J. Hazard. Mater.*, *188*(1), 29–36.

Yan, J., & Li, L. (2013). Multi-objective optimization of milling parameters – the trade-offs between energy, production rate and cutting quality. *J Clean Prod*, *52*, 462–471.